

07.04

Variation of the micromechanics of impact fracture of MgAl_2O_4 in response to the applied hot isostatic pressing

© I.P. Shcherbakov¹, E.V. Afanaseva², A.A. Dunaev³, S.B. Eronko², A.G. Kadomtsev¹,
M.V. Narykova¹, A.E. Chmel^{1,¶}

¹ Ioffe Institute,
St. Petersburg, Russia

² Peter the Great Saint-Petersburg Polytechnic University,
St. Petersburg, Russia

³ Vavilov State Optical Institute,
St. Petersburg, Russia

¶ E-mail: chmel@mail.ioffe.ru

Received May 12, 2022

Revised May 12, 2022

Accepted May 14, 2022

The MgAl_2O_4 ceramics produced by the preliminary clinkering of synthesized powder was exposed to the hot isostatic pressing (HIP). Samples were subjected to a pointed impact loading, which excited the acoustical and electromagnetic emissions (AE and EME, respectively). In non-HIP-treated samples, the energy distribution in time series of AE and EME pulses followed an exponential law, while after an application of the hot isostatic pressing procedure, the emissions of both types exhibited the power law energy distributions in time sweeps. A variation of the specificity of the impact-induced AE/EME energy release was explained by a transition from the nucleation/decay of microcracks in non-HIP-treated ceramics to the self-organized dislocation folding directed to grain boundaries in the material characterized by the density that was close to that of a MgAl_2O_4 single crystal.

Keywords: MgAl_2O_4 ceramics, hot isostatic pressing, impact loading, acoustic emission, electromagnetic emission.

DOI: 10.21883/PSS.2022.10.54239.377

1. Introduction

Ceramics made of magnesium aluminate spinel (MAS) MgAl_2O_4 is a polycrystalline material of high strength, sufficient for use in personal protective equipment for people and equipment from point mechanical influences as a substitute for heavy, thick metal products [1]. Due to the transparency in the spectral region of 0.2–5.5 μm , MAS ceramics are also used to create protective screens of optical devices on external devices [2], where they are exposed to blows of solid dust particles and precipitation [3]. The cubic crystal structure makes the MAS optically isotropic, which eliminates the proportion of scattered light associated with the birefringence effect.

In the industry, MAS is produced from finely dispersed powder by hot pressing/sintering at temperatures up to 1500–1600 °C and a pressure of 100–200 MPa. However, such treatment does not eliminate small pores in ceramics, which significantly reduce transparency. An effective means of increasing the density of the material is hot isostatic pressing (HIP) of products, at which the density can reach 99.94% of the theoretical density [4].

In the proposed study, the micromechanical aspect of the change in the specific features of the destruction of MAS as a result of the application of the finishing of the material with the HIP procedure was considered. In accordance with the above-mentioned spinel application, the tests were

carried out by spot impact damage to the surface of the samples. On impact, time-based sweeps of acoustic emission (AE) and electromagnetic emission (EME) signals were recorded, and the parameters of the MAS response to mechanical stress before and after HIP processing were compared.

2. Samples and equipment

The initial powdered raw material MgAl_2O_4 for the production of ceramic samples was prepared by sol-gel synthesis (Pechini method [5]), in which the polymeric material obtained from metal salts, polybasic acids and polyatomic alcohol were calcined at temperatures up to 1000 °C. To prevent strong agglomeration and sintering of particles [6] additional heat treatment was applied in the melt of potassium chloride. Then hot vacuum single-axis pressing of the powder (hot pressing, HP) was carried out at a pressure of 150 MPa and a temperature of 1250 °C for 30 min. Isostatic heating was carried out in an argon atmosphere at a pressure of also 150 MPa and a temperature of 1275 °C for 100 min.

Measurement of the density of the sample was carried out by hydrostatic weighing on the analytical balance Simadzu AUW 120D using the prefix SMK-301. For the precision

Table 1. The density and microhardness of MgAl₂O₄ ceramics before and after HIP application

Density, g/cm ³		Microhardness V _h , GPa	
Before HIP processing	After HIP processing	Before HIP processing	After HIP processing
3.550±0.002	3.559±0.002	17.89±0.16	19.16±0.55

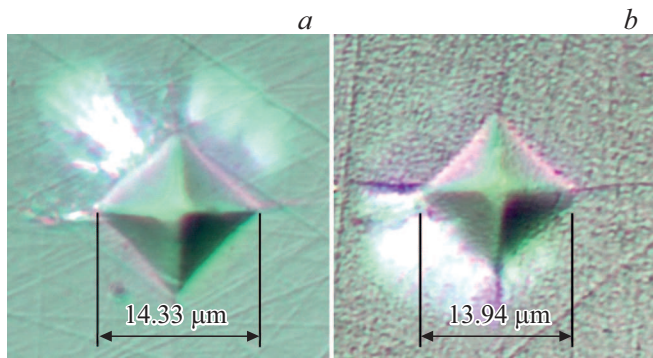


Figure 1. Photos of Vickers pyramid prints on the MAS plate before (a) and after (b) the HIP application.

determination of density, samples with a mass of the order of 1.5 g were used, distilled water was used as a liquid.

The microhardness of the samples was measured on the PMT-3 instrument using an Axio Vert.A1 microscope equipped with a Carl Zeiss Axiocam 208 color digital camera. Prints were made using the Vickers pyramid at a load of 200 g (1.96 N) and a shutter speed of 10 s. Figure 1 shows photographs of characteristic prints in the sample before (a) and after (b) isostatic exposure to temperature and pressure.

Damage to the samples, made in the form of polished discs with a diameter of 20 mm and a thickness of 1 mm, was caused by the impact of a load falling on a steel barrel placed on the sample. When impacted on its surface, signals of acoustic emission (AE) and electromagnetic emission (EME) were recorded. The broadband AE detector, made of highly sensitive piezoceramics Pb(Zr_xTi_{1-x})O₃, recorded a signal in the frequency band of 80–500 kHz, which excluded the low-frequency effect of oscillations of the experimental unit. EME was recorded using a Hertz dipole; the most intense EME radiation was observed in the band of 600–900 kHz. EME and AE signals were received at the input of the analog-to-digital converter ASK-3106 and in digital form were stored in a computer. The temporal resolution of the pulses was 20 ns.

3. Results

Changes in the density and microhardness of the material after isostatic processing are given in Table 1. The relative

error in determining the density of $\Delta\rho/\rho$ was 0.02%. The increase in microhardness exceeded 7%.

The results of the application of emission methods to assess the effect of HIP on the dynamic destruction of MAS are presented in the form of time series of AE and EME pulses induced by the impact of the striker (Fig. 2) with the subsequent analysis of the distributions of the allocated energy in pulses. The energy E allocated in an AE or EME pulse is proportional to the square of the pulse amplitude: $E \propto A^2$. It can be seen that the duration of sound emission in a sample that has not been subjected to isostatic heating (Fig. 2, a) is significantly lower than the duration of the signal from the sample that underwent the HIP procedure (Fig. 2, b). And the latter does not have a pronounced peak.

The EME signal sweeps in the non-HIP samples had a greater extent than the AE sweeps, but did not extend beyond 1 ms. In addition, repeated repetition of the experiment showed that the peak of EME radiation in samples before HIP processing was always delayed relative to the peak of AE by about 200 μs (cf. Fig. 2, a and 2, b). After isostatic processing, the EME signal in repeated experiments manifested itself randomly with respect to the time of emission of AE, which had a much longer duration than before isostatic processing. In some cases, the EME sweep involved 2–3 „flashes“, as the example in Fig. 2, d shows.

The regularities of energy release in a series of pulses were determined by constructing distributions of the number of pulses of one type or another in the form of dependencies $N(E > \epsilon)$ versus ϵ , where the number of pulses N is deposited at the vertical coordinate, the energy of which E is higher than the value ϵ , which receives a number of energy values in the pulses that came during the registration of the signal (horizontal coordinate). Figure 3, a, b shows the energy distributions in shock-induced pulses of AE and EME emitted from the sample prior to HIP processing. The graphs are constructed in semilogarithmic coordinates, in which the experimental points, both AE and EME, are stacked on line segments with a slope of a :

$$\log_{10} N(E > \epsilon) \propto -a\epsilon. \tag{1}$$

Correlation (1) is equivalent to the Poisson-type exponential law:

$$N(E > \epsilon) \propto \exp(-a\epsilon), \tag{1a}$$

which describes the distribution of random events that occur independently of each other.

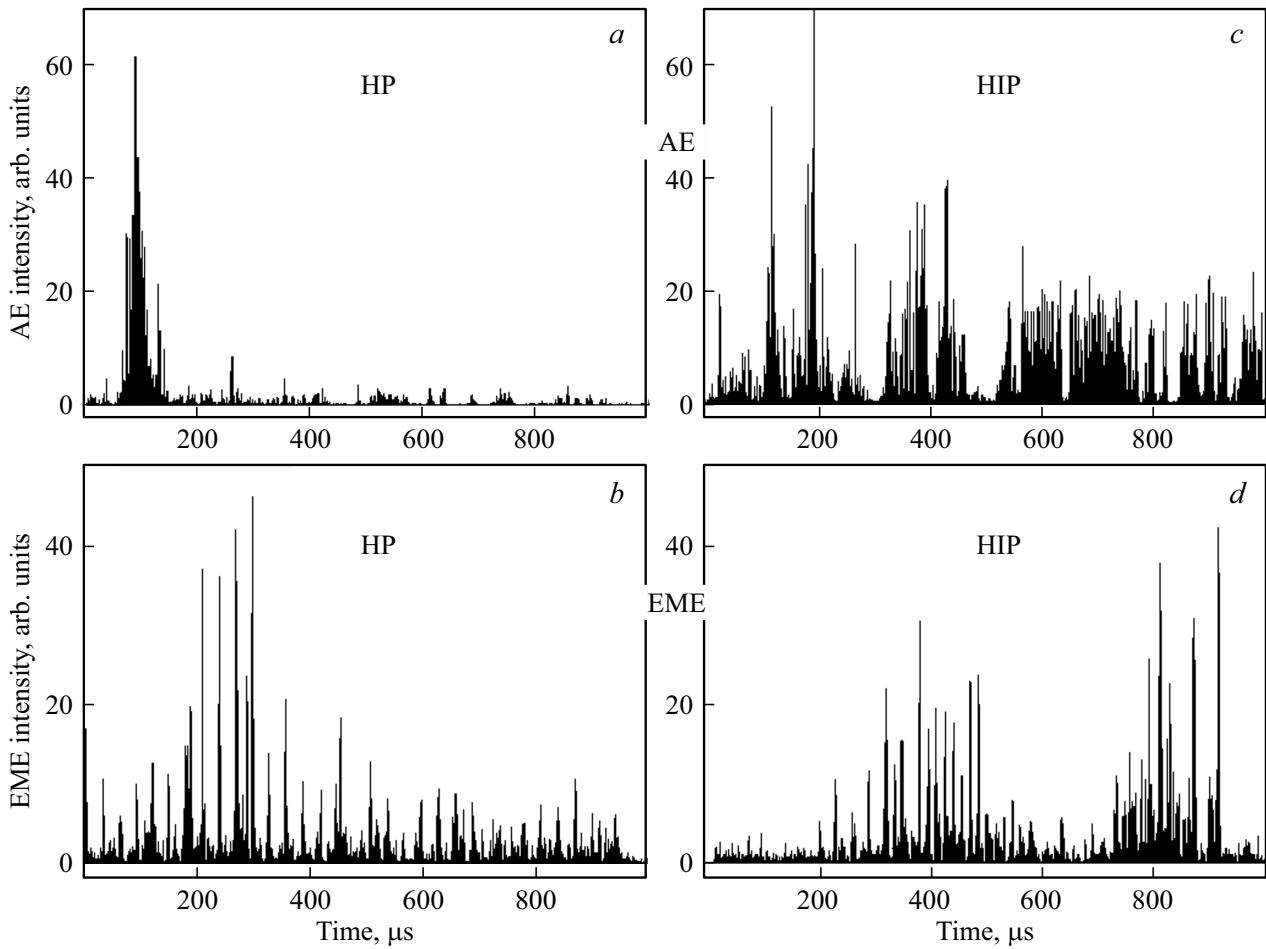


Figure 2. Sweeps of shock-triggered signals of AE (*a, c*) and EME (*b, d*) for samples after hot pressing HP (*a, b*) and after additional exposure HIP (*c, d*).

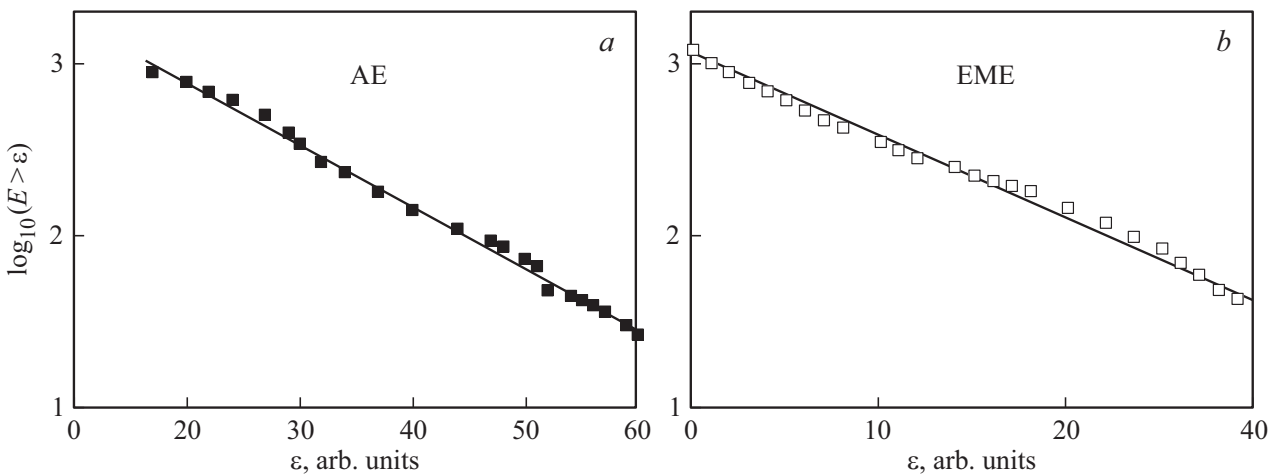


Figure 3. The energy distributions in pulses of AE (*a*) and EME (*b*) calculated from the time series for samples up to HIP exposure shown in Fig. 2, *a, b*.

The same graphs $N(E > \epsilon)$ *versus* ϵ were built for the samples after they passed the HIP procedure (Fig. 4, *a, b*). It can be seen that the energy distributions in the emissions

of both types did not show linear plots in semilogarithmic coordinates, that is, they did not follow the exponential law of the equation type (1a). The same graphs were rearranged

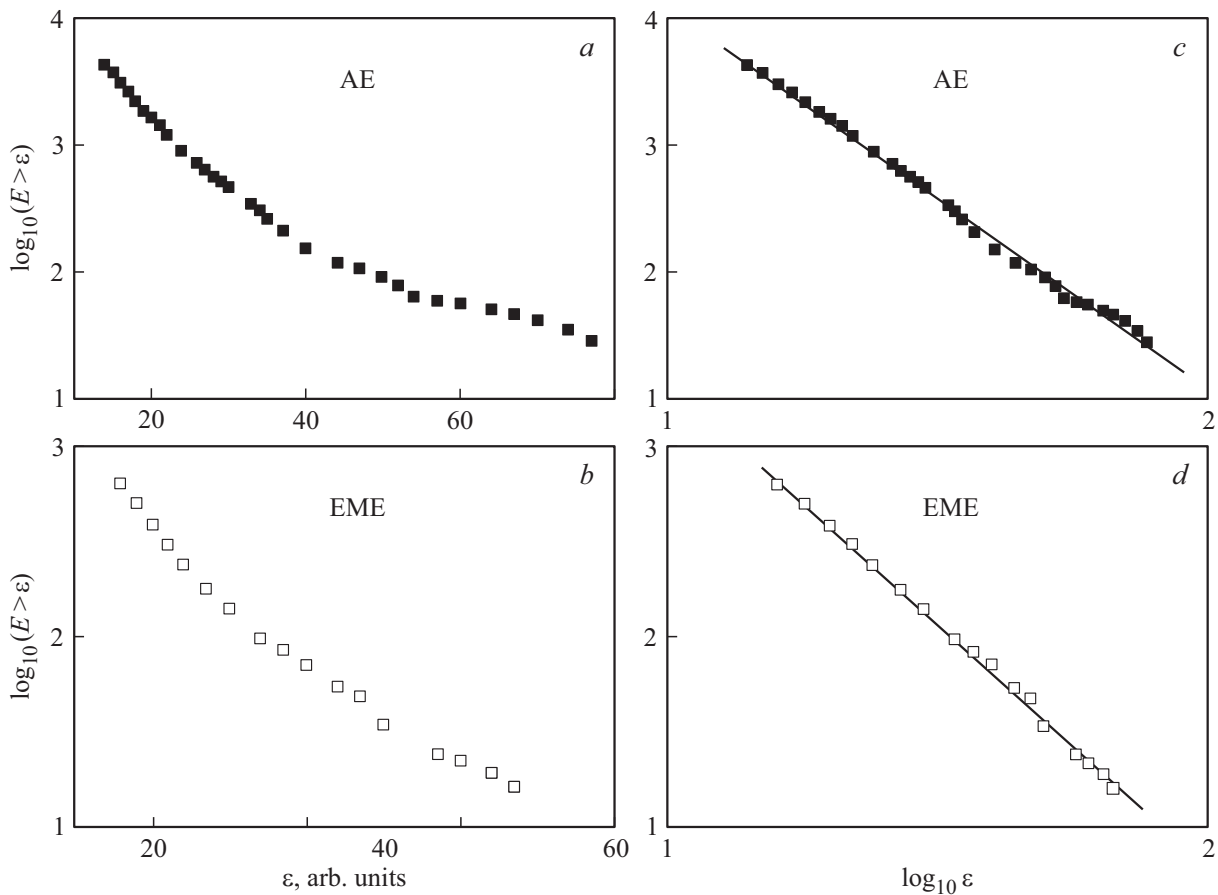


Figure 4. The energy distributions in pulses of AE (*a, c*) and EME (*b, d*) calculated from the time series for HIP samples, represented in semi-logarithmic (*a, b*) and double logarithmic (*c, d*) coordinates.

Table 2. The effect of HIP processing on the nature of energy distributions in AE and EME pulses

Before HIP processing	After HIP processing
In untreated by HIP material, the AE signal is shorter than the EME signal, and the peak of the latter is delayed relative to the peak of AE. Energy output in time series of pulses of both types before isotactic processing followed an exponential law characteristic of random events.	The duration of emission activity is significant increased, and EME radiation occurs randomly against the background of the flow of AE. The energy distribution of the AE and EME pulses was described by power law typical of correlated processes, when the occurrence of a single event affects the probability of the occurrence of the following due to long-range interaction

in double logarithmic coordinates (Fig. 4, *c, d*), where log-linear segments appeared

$$\log_{10} N(E > \epsilon) \propto -b \log_{10} \epsilon, \tag{2}$$

equivalent to a power law

$$N(E > \epsilon) \propto \epsilon^{-b}. \tag{2A}$$

Thus, after the treatment of MAS by means of HIP, the qualitative nature of the emission activity has changed. Acoustic and electromagnetic radiation was manifested by the power law of energy distribution, which is characteristic of correlated, self-organized processes

4. Discussion

The study revealed a number of changes in the emission activity excited by the blow in the MAS after high-temperature isostatic pressing of the sample. Let's formulate them in Table 2.

A change in the duration and mutual arrangement of the AE and EME time series relative to each other indicates a change in the micromechanical behavior of MAS as a result of HIP processing. To interpret the result obtained, we turn to the data obtained in the studies of acoustic and electromagnetic radiation from geomaterials

that, like ceramics, have a high heterogeneity. Laboratory experiments and field observations during earthquakes and mountain impacts have a long history in geophysics. The variability of the parameters of the registered AE and EME led to the emergence of two models describing the micromechanics of rock destruction during various tectonic phenomena. The technique consists in the following. When a shock wave passes, microcracks appear in the rocks, the appearance of which is accompanied by acoustic emission. At the same time, electric charges of the opposite sign are formed on the crack edges. After the passage of the shock wave, a significant proportion of cracks relax, and the charges on the closed walls annihilate — the EME effect occurs [7].

However, not all forces generate the appearance of discontinuities with open surfaces. Depending on the physical and mechanical properties of the rock and the nature of the current pressure, sliding of the fragments of the array relative to each other may occur. In laboratory experiments simulating this process, it was shown that during dynamic contact of natural non-smooth surfaces, electromagnetic radiation is generated in a wide range — up to the visible glow [8].

We believe that in our experiments with MAS, both mechanisms have manifested themselves. As mentioned above, only isostatic pressing allows the smallest pores to be removed from the ceramics. The density of the material before HIP is insufficient to exclude the formation of open microcracks during the passage of a shock wave in a heterogeneous material. The relaxation of the cracks after the peak load caused rapid annihilation of electrical charges. Both emission effects were short-lived (up to several hundred microseconds) and had a clear sequence.

The density of HIP-treated ceramic MAS is close to the density of a single crystal $MgAl_2O_4$ [4]. This may explain the absence of open microcracks that relax after impact. At the same time, the ultra-high compaction of the MAS by pressure leads to the formation of dislocations [9]. The contact of the striker with the surface caused a cooperative movement of dislocations with access to the grain boundaries, which was accompanied by the generation of AE and EME [10].

This mechanism for the compacted HIP MAS is confirmed by the power-law distribution of energy in the AE and EME pulses, obtained in this study (Fig. 4, *b*), which is characteristic of the self-organized behavior of the dislocation ensemble [11].

The authors [8] also noted the power distribution of energy in EME pulses during friction of granite samples, but did not indicate the cause of the effect.

5. Conclusion

AE and EME methods have shown that the holding of $MgAl_2O_4$ ceramics under isostatic pressure at high temperature (HIP) led to a change in the mechanism

of transmission of shock energy to the tested material. The formation of microcracks with the AE effect and the subsequent EME radiation after the passage of the shock wave as a result of the annihilation of electric charges that arose on the cracks edges were observed only on non-exposed HIP samples. The nucleation and collapse of cracks was characterized by a random (exponential) law. Isostatic processing led to an increase in the density of ceramics to 98% of the value in a single crystal, that is, to the almost complete removal of microstrings that could serve as centers for the origin of microcracks under shock load. The energy distributions in the time series of both AE and EME were self-similar (powered), which occurs in the ensemble of dislocations as they move.

Conflict of interest

The authors declare that they have no conflict of interest.

References

- [1] C. Gajdowski. Thèse pour obtenir le grade de Docteur. Université de Valenciennes et du Hainaut-Cambresis, NNT: VALE0022 (2018).
- [2] M. Ramisetty, S. Sastri, U. Kashalikar, L.M. Goldman, N. Nag. *Am. Ceram. Soc. Bull.* **92**, 20 (2013).
- [3] G.H. Jilbert, J.E. Field. *Wear*. **243**, 6 (2000).
- [4] D.S. Tsai, C.T. Wang, S.J. Yang. *Mater. Manuf. Proc.* **9**, 709 (1994).
- [5] D.V. Tolstikova, E.V. Golyeva, V.S. Lebanin, M.D. Mikhailov, A.A. Dunaev, V.N. Vetrov, B.A. Ignatenkov. *Opt. zhurn.* **81**, 69 (2014) (in Russian).
- [6] D.V. Tolstikova, M.D. Mikhailov, V.M. Smirnov. *Zhurn. obshchei khimii* **84**, 1744, (2014) (in Russian).
- [7] K.A. Eftaxias, V.E. Panin, Ye.Ye. Deryugin. *Tectonophys.* **431**, 273 (2007).
- [8] J. Muto, H. Nagahama, T. Miura, I. Arakawa. *Tectonophys.* **431**, 113 (2007).
- [9] C.W. Zh. Zhao. *Scripta Materialia* **61**, 193 (2009).
- [10] B.Ts. Manzhikov, L.M. Bogomolov, P.V. Ilyichev, V.N. Sychev. *Geol. Geofiz.* **10**, 1690 (2001) (in Russian).
- [11] G.A. Malygin. *UFN* **169**, 979 (1999) (in Russian).